

CORRELATION BETWEEN GAS AND LIQUID PERMEABILITY WITH NOISE REDUCTION COEFFICIENT IN INSULATION BOARDS MADE FROM SUGAR CANE BAGASSE

HAMID REZA TAGHIYARI¹; ABDOLLAH ELYASI²; KAZEM DOOST-HOSEINI²; REZA HOSSEINPOURPIA^{*3,4}

¹Shahid Rajaee Teacher Training University, Faculty of Civil Engineering, Wood Science and Technology Department, 2122970021 Iran

²University of Tehran, Faculty of Natural Resources, Wood and Paper Sciences and Technologies Department, 2632249311 Iran

³Linnaeus University, Department of Forestry and Wood Technology, Lückligrads plats 1, 351 95 Växjö, Sweden

⁴Georg August University Göttingen, Burckhardt Institute, Department of Wood Biology and Wood Products, Büsgenweg 4, 37077 Göttingen, Germany

Abstract

Taghiyari, H. R., A. Elyasi, K. Doost-Hoseini and Reza Hosseinpourpia, 2017. Correlation between gas and liquid permeability with noise reduction coefficient in insulation boards made from sugar cane bagasse. *Bulg. J. Agric. Sci.*, 23 (3): 674–681

Specific gas and liquid permeability, as well as noise reduction coefficients, in insulating boards made of sugar-cane bagasse were studied here. Urea-formaldehyde (UF) and melamine-urea-formaldehyde (MF) were used to produce homogeneous as well as three-layered insulating boards with three densities of 0.3, 0.4, and 0.5 g/cm³. The obtained results indicated that MF slightly decreased gas and liquid permeability, but it did not significantly affect the noise reduction coefficients. Gas and liquid permeability were considerably affected by the density of the boards, due to the compression between the bagasse particles and less spaces and voids to let the fluids to pass through. However, noise reduction coefficients were significantly affected both by the density, as well as the board-type. More compression between the particles and the consequent less space between the bagasse particles entangled the waves; furthermore, the sudden change between the layers in the three-layered boards formed a barrier towards transmission of waves.

Key words: bagasse; insulation board; noise reduction coefficient (NRC); permeability; sound absorption; sugarcane

Introduction

Wood is frequently modified by engineering processes to give stiffness or homogeneous mechanical properties (Awotemi, 2007; Tsuchikawa, 2007; Taghiyari et al., 2011; Taghiyari, 2012) as well as resistance to wood-deteriorating agents (Taghiyari et al., 2014) because few species offer radial and axial uniformity in their produced wood (Taghiyari and Malek, 2014), the quality of wood can be affected by rotation period, mono- or mixed-species cultivation, light and soil, initial spacing, as well as interaction between clone-type and site (Acre and Moya,

2015). Composite-boards, however, offer the advantages of a homogeneous structure and the use of raw materials without restrictions as to the shape and size (Grace, 2005). In this connection, the majority of humans world-wide depend upon wood products harvested from forests; therefore, efficient use of agricultural residues is a desirable goal from both environmental and economic standpoints (Grace, 2005). Agro-based particle-boards are manufactured from various lignin-cellulosic materials, usually wooden and mainly in the particle form, which are combined with an adhesive that consolidates under the action of temperature and pressure (Rowell et al., 2000). The main fac-

*Corresponding author: reza.hosseinpourpia@lnu.se

tors that influence the properties and quality of the panels are the density of the panel, geometry, and moisture content of the particles, the pressing cycle, and the quantity and type of adhesive and many studies have been carried out to promote the quality of the resin and boards (Maloney, 1993; Kelly, 2007; Stockel et al., 2012; Valenzuela et al., 2012).

Use of agricultural fibers in building products represents a high-value application, in comparison to the common use as fuel or mulch. Bagasse fiber performs similarly to hardwood fiber in composite board products, and there has been considerable interest in developing such products (Grace, 2005). This interest has run the gamut from cheaply produced products for local construction use (Grace, 1996) to more refined and dimensionally stable fiberboards (Rowell and Keanny, 1991) and particleboards (Wu, 2003; Youngquist et al., 1996). Sugarcane, a very tall grass with big stems, is largely grown in countries like Brazil, Cuba, Australia, South Africa, Peru, Mexico, and India (Ripoli et al., 2000). Bagasse, or sugarcane rind, is a fibrous by-product of sugar extraction from sugarcane, *Saccharum officinarum* L. Another kind of bagasse, coconut bagasse, is also used in the industry (Panyakaew and Fotios, 2011; Sousa et al., 2012). Sugarcane bagasse consists of cellulose 43.8%, hemicellulose 28.6%, lignin 23.5%, ash 1.3%, and other components 2.8% (Luz et al., 2007). The two former components are hydrophilic, and the latter is hydrophobic (Sun et al., 2004). Bagasse fiber performs similarly to hardwood fiber in composite board products; thus, it could be very important for countries that lack of wood fiber (Rainey et al., 2009). However, only a very small portion of the bagasse is reused to produce high-valued product, such as paper and bio-based products (Lei et al., 2010). In fact, sugarcane bagasse is considered either as a waste, affecting the environment, or as a resource when appropriate valorization technologies are implemented (Pereira et al., 2011). Sugarcane bagasse, in combination with coconut husk, has also had promising results in the production of thermal insulation boards (Panyakaew and Fotios, 2011).

There are vast sources for sugarcane bagasse in the Southern parts of Iran; therefore, the use of bagasse in the production of sound absorbing insulation boards with different densities as well as using two different resins was studied here to evaluate the results of resin-type as well as density in particleboards made of sugar cane bagasse. Furthermore, due to the importance of gas and liquid permeability as two main physical properties in wood and wood composites, the correlations between

the noise reduction coefficients at different frequencies with the liquid and gas permeability of the boards were also evaluated.

Materials and Methods

Specimen Procurement

The bagasse fibers were procured from Imam Khomeini Farms located in Shooshtar city in the Southern parts of Iran. They were dried with a rotary dryer for 90 minutes to the final moisture content of 2%. The temperature of the drier was about 70°C. Once dried, they were put in plastic bags and sealed. For homogeneous boards, no separation was made in the fibers; however, for multi-layered boards, fibers were passed through laboratory sieves to be separated into two groups of small- and large-sized fibers.

Urea-formaldehyde (UF) and melamine-urea-formaldehyde (MUF) were procured from Siran-Chemistry Factory in Iran. Specifications of the resins used are summarized in Table 1. For all treatments and both resins, the resin-content was 12%, based on the dry-weight basis of the fibers. Chloride ammonium (1%) was used as catalyst.

Both homogeneous as well as multi-layered boards were produced with three densities of 0.3, 0.4, and 0.5 g/cm³. Moisture content (MC) of the mat was 10%. A Burkle-LA 160 laboratory hot press was used to produce the boards. Specific pressure of the plates was 15 kg/cm²; total nominal pressure of the plates was 100 kgf. Temperature of the hot-press plates were fixed at 170°C. The press time of all treatments was fixed at 4 minutes. Thickness of all boards was controlled by stopper bars to be fixed at 12 mm. In total twelve treatments were produced; for each treatment, five replications were made. Boards were kept in the conditioning chamber (30°C, and 40–45% relative humidity) for two months before the tests were carried out on them. Moisture content of the specimens was 8.5% at the time of all measurements.

Gas Permeability Measurement

Longitudinal gas permeability measurement was carried out by an apparatus with milli-second precision designed and built by the first author based on the microstructure porosity of wood (Figure 1) (USPTO No. 8,079,249 B2) (Taghiyari and Malek, 2014). Falling water volume displacement method was used to calculate specific longitudinal gas permeability values (Taghiyari and Malek, 2014). Connec-

Table 1

Specifications of the urea formaldehyde and melamine urea formaldehyde resins

Resin type	Density (g/cm ³)	Solid (%)	pH	Viscosity (cP)	Gel time (s)
Urea formaldehyde (UF)	1.25	59	6.8 – 7.1	200 – 240	50 – 65
Melamine urea formaldehyde (MUF)	1.225	56	8 – 9	90 – 100	70 – 80

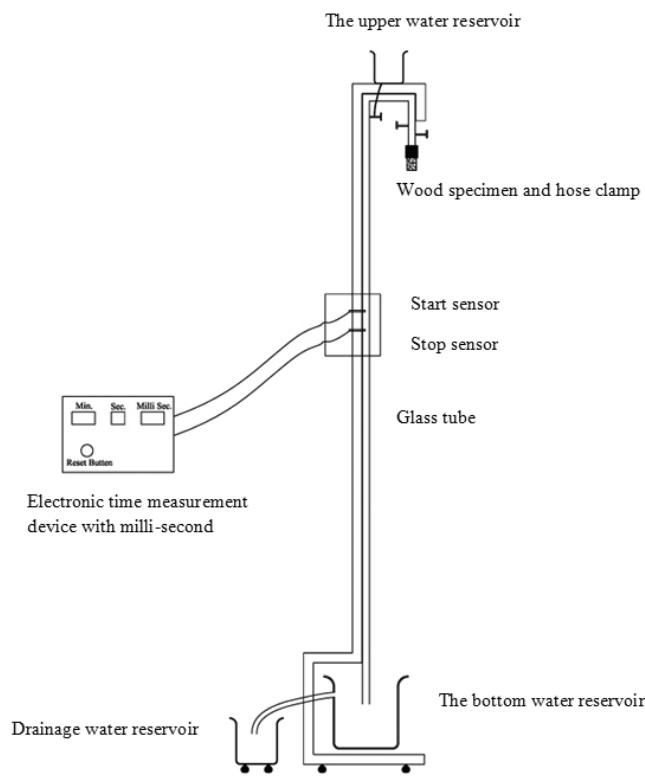


Fig. 1. The overview of the gas permeability apparatus equipped with milli-second precision electronic time measurement device (USPTO No. 8,079,249 B2; Pub No. 2010/0281951) (Approved by The Iranian Research Organization for Scientific and Technology under certificate No. 47022)

(Taghiyari & Moradi Malek 2014)

tion between the specimen and holder of the apparatus was made fully air-tight, using silicone hose and silicon grease. A pressure gauge with milli-bar precision was connected to the whole structure to monitor pressure gradient (ΔP) and vacuum pressure at any particular time as well as height of

Table 2

Vacuum pressures at starting and stopping points for each of the 7 measuring heights

Code of the 7 Water Columns	Height of the 7 Water Columns at Starting Point (cm)	Height of the 7 Water Columns at Stopping Point (cm)	Starting point vacuum pressure (minus milli-bar)	Stopping point vacuum pressure (minus milli-bar)
Gas 1	149.5	139.5	155	146.5
Gas 2	134.5	124.5	141.5	132
Gas 3	119.5	109.5	126.5	117
Gas 4	104.5	94.5	112	101.5
Gas 5	89.5	79.5	97.5	86.5
Gas 6	74.5	64.5	82	72
Gas 7	59.5	49.5	66.5	56

water column (Table 2). A total of 300 cylindrical specimens with 29.9 mm in diameter and 12 mm in thickness were randomly cut at scattered locations from each board for specific gas permeability, as well as liquid permeability and NRC.

Three time measurements were taken for each specimen with milli-second precision (Taghiyari et al., 2012). Superficial permeability coefficient was then calculated using Siau's Equations (Equations 1 and 2) (Siau, 1995). The superficial permeability coefficients were then multiplied by the viscosity of air ($\mu=1.81\times10^{-5}$ Pa s) to obtain the specific permeability ($K=k_g \mu$).

$$k_g = \frac{V_d CL(P_{atm} - 0.074\bar{z})}{tA(0.074\bar{z})(P_{atm} - 0.037\bar{z})} \times \frac{0.760 \text{ mHg}}{1.013 \times 10^6 \text{ Pa}} \quad (1)$$

$$C = 1 + \frac{V_r(0.074\Delta z)}{V_d(P_{atm} - 0.074\bar{z})}, \quad (2)$$

where: k_g = longitudinal specific permeability ($\text{m}^3 \text{ m}^{-1}$); $V_d = \pi r^2 \Delta z$ [r = radius of measuring tube (m)] (m^3); C = correction factor for gas expansion as a result of change in static head and viscosity of water; L = length of wood specimen (m); P_{atm} = atmospheric pressure (m Hg); \bar{z} = average height of water over surface of reservoir during period of measurement (m); t = time (s); A = cross-sectional area of wood specimen (m^2); Δz = change in height of water during time t (m); V_r = total volume of apparatus above point 1 (including volume of hoses) (m^3)

Liquid Permeability Measurement

Liquid permeability was measured using Rilem test tube II.4 (Taghiyari and Malek, 2014) according to Rilem Commission 25, PEM, Test Method 1154 by the International Union of Laboratories and Experts in Construction Materials, Systems, and Structures; penetration tests were carried out under laboratory conditions according to ASTM E-514 (Figure 2). Two times were measured: 1 – The time the first drop of water falls off the bottom surface of the specimens; 2 – The time the level of water in Rilem tube lowers by 50-mm in the tube (that is, 6.6 CC of water). Relationship between gas time values and the two liquid permeability time values was then calculated.

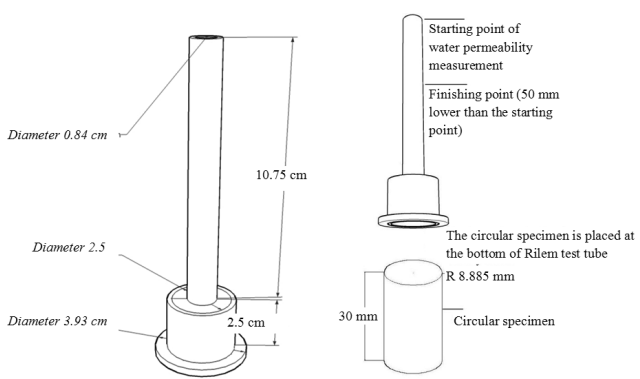


Fig. 2. Liquid permeability measurement apparatus (Rilem test tube)

(Taghiyari & Moradi Malek 2014)

Noise reduction coefficient measurement

Noise reduction coefficient (NRC) was carried out in accordance to DIN-68763; five different frequencies of 250, 500, 1000, 2000, and 4000 Hz were measured for each single specimen, using standing wave apparatus type 4002, sine random generator type 1024, and beat frequency oscillator type 1022.

Statistical Analysis

Two-way analysis of variance (ANOVA) was performed, using SAS software program, version 9.1 (2003), to discern

Table 3

Regression analysis of the 7 gas permeability time values of different water column heights with liquid permeability time values (1st drop and 50-mm-lowering) for all the 12 treatments in the present study

Gas and Water Permeabilities	Gas 1	Gas 2	Gas 3	Gas 4	Gas 5	Gas 6	Gas 7
1 st Drop	0.953 ** (+)	0.890 ** (+)	0.954 ** (+)	0.938 ** (+)	0.958 ** (+)	0.941 ** (+)	0.955 ** (+)
50-mm Lowering time	0.909 ** (+)	0.978 ** (+)	0.892 ** (+)	0.906 ** (+)	0.906 ** (+)	0.895 ** (+)	0.896 ** (+)
Gas 1	1 0.861 ** (+)	0.967 ** (+)	0.991 ** (+)	0.994 ** (+)	0.994 ** (+)	0.994 ** (+)	0.995 ** (+)
Gas 2	1 0.815 ** (+)	0.862 ** (+)	0.846 ** (+)	0.850 ** (+)	0.838 ** (+)	0.838 ** (+)	0.838 ** (+)
Gas 3		1 0.950 ** (+)	0.986 ** (+)	0.951 ** (+)	0.978 ** (+)	0.978 ** (+)	0.978 ** (+)
Gas 4			1 0.985 ** (+)	0.989 ** (+)	0.981 ** (+)	0.981 ** (+)	0.981 ** (+)
Gas 5				1 0.988 ** (+)	0.997 ** (+)	0.997 ** (+)	0.997 ** (+)
Gas 6					1 0.991 ** (+)	0.991 ** (+)	0.991 ** (+)
Gas 7						1	

** Statistically significant at the 1 % level.

Gas 1 – 7: The 7 water column heights for measuring gas permeability representing the 7 vacuum pressures

(+) Positive correlation

significance difference at 95% level of confidence. Regression and hierarchical cluster analysis, including dendrogram and using Ward methods with squared Euclidean distance intervals, were carried out by SPSS/16 (2007). Cluster analysis was carried out to determine potential similarities between various treatments based on more than one property simultaneously. Cluster analysis has the potential to evaluate the groupings on the basis of more than two properties in a single run. The scaled indicator in each cluster analysis demonstrates which treatments are similar or different; lower scale numbers show more similarities while higher ones show dissimilarities (Ada, 2013).

Results and Discussion

Regression analysis between the seven gas permeability time values with the two liquid permeability time values indicated that there were high R-square for all the seven vacuum pressure (Table 3); high correlations were also found between the seven vacuum pressures. However, the highest correlation was found between the 5th gas permeability with the two liquid permeability times; therefore, specific gas permeability of this vacuum pressure was reported here. Specific gas permeability decreased as the density of the boards increased (Figure 3).

The highest specific gas permeability was found in the homogeneous board with 0.3 g/cm³ of density, using UF-

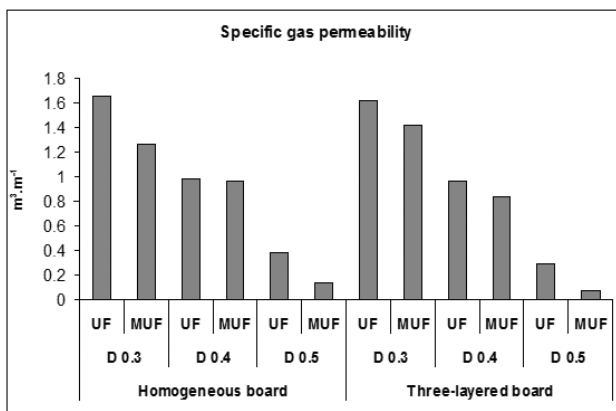


Fig. 3. Specific gas permeability for the 12 treatments in the present study (UF = Urea Formaldehyde resin; MUF = Melamine Urea Formaldehyde resin; D = Density) ($\times 10^{-11} \text{ m}^3 \cdot \text{m}^{-1}$)

resin ($1.660 \times 10^{-11} \text{ m}^3 \cdot \text{m}^{-1}$), and the lowest was observed in 3-layered boards with 0.5 g/cm^3 of density, using MUF-resin ($0.074 \times 10^{-11} \text{ m}^3 \cdot \text{m}^{-1}$). As to the more compression between the bagasse particles in the board-matrix of higher density boards, this decreasing trend can be justified. Furthermore, boards with MUF-resin tended to have less permeability comparing with their equivalent boards with UF-resin. The multi-dimensional ultra-structure of MUF-resin can explain the decreasing effect it had on the gas permeability. Similar decreasing trend in liquid permeability was also observed in both liquid permeability values, that is, 1st-Drop and 50-mm lowering times (Figures 4 and 5). The lowest liquid permeability times (the highest time values) were found in the three-layered boards with 0.5 g/cm^3 of density and MUF-resin (28.65 and 66.90 seconds for 1st-Drop and 50-mm lowering times); this treatment also showed the lowest gas permeability between the 12 treatments. MUF-resin also tended to result in lower liquid permeability in most of the treatments. The high R-square between the specific gas permeability and the liquid permeability time values proved that the non-destructive test of gas permeability measurement can be a suitable substitute for prediction of liquid permeability behavior in the sugar-cane particleboards.

Regression analysis between the specific gas and liquid permeability, with the noise reduction coefficients (NRCs) showed significant correlations only in two frequencies of 500 and 2000 Hz (Table 4). The highest noise reduction coefficient was found in the three-layered boards with 0.5 g/cm^3 of density and UF-resin, tested at the frequency of 2000 Hz (0.89), and the lowest in homogeneous boards with 0.5 g/cm^3 of density and UF-resin tested at 500 Hz (Figure 6). The

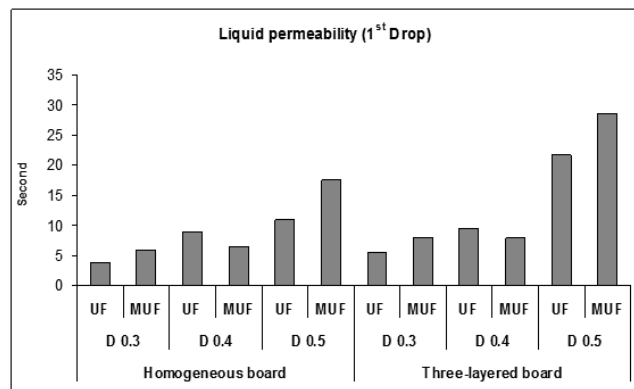


Fig. 4. Liquid permeability of 1st-Drop (second) for the 12 treatments in the present study (UF = Urea Formaldehyde resin; MUF = Melamine Urea Formaldehyde resin; D = Density)

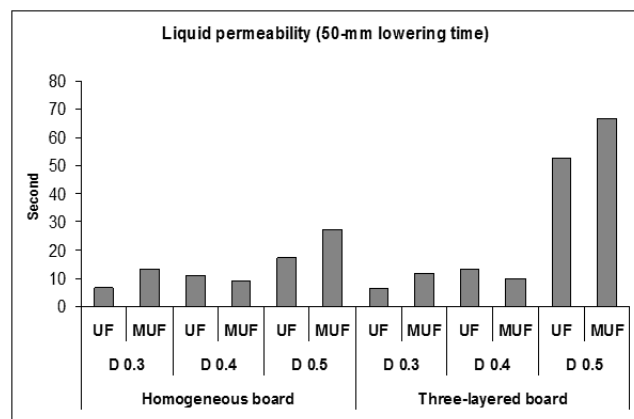


Fig. 5. Liquid permeability of 50-mm lowering time (second) for the 12 treatments in the present study (UF = Urea Formaldehyde resin; MUF = Melamine Urea Formaldehyde resin; D = Density)

higher frequency of 2000 Hz clearly resulted in more noise absorption, showing that higher frequencies may be more easily entangled in the pores and voids of the particleboard; furthermore, noise absorption generally decreased with the increase in density. Only three-layered boards with UF-resin showed an increasing trend in noise absorption as the density increased, at both at the frequencies of 500 and 2000 Hz.

Cluster analysis of the 12 treatments based on the specific gas permeability as well as the two liquid permeability times showed that all treatments with the same density of either 0.3 or 0.4 g/cm³ were clustered quite closely (Figure 7A). This may indicate that in the lower density boards (0.3 and 0.4 g/

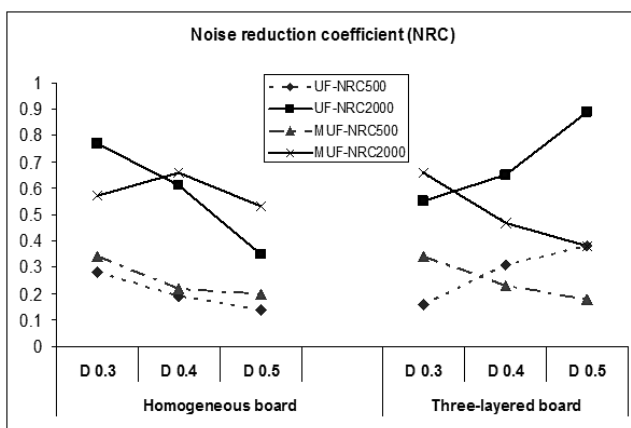


Fig. 6. Noise reduction coefficients for the 12 treatments in the present study at 500 and 2000 Hz frequencies (UF = Urea Formaldehyde resin; MUF = Melamine Urea Formaldehyde resin; D = Density)

Table 4

Regression analysis of the 7 gas permeability time values of different water column heights with liquid permeability time values (1st drop and 50-mm-lowering) for all the 12 treatments in the present study

Properties	R-square				
	NRC-250	NRC-500	NRC-1000	NRC-2000	NRC-4000
Specific gas permeability (Gas 5)	.122	.640	.452	.609	.336
	NS (-)	* (+)	NS (+)	* (+)	NS (+)
Liquid permeability (1 st -Drop)	.153	.549	.219	.631	.161
	NS (+)	* (-)	NS (-)	* (-)	NS (-)
Liquid permeability (50-mm lowering time)	.207	.460	.177	.581	.125
	NS (+)	NS (-)	NS (-)	* (-)	NS (-)

* Statistically significant at the 5 % level.

NS Not Significant.

(+) positive (+) or negative (-) correlation

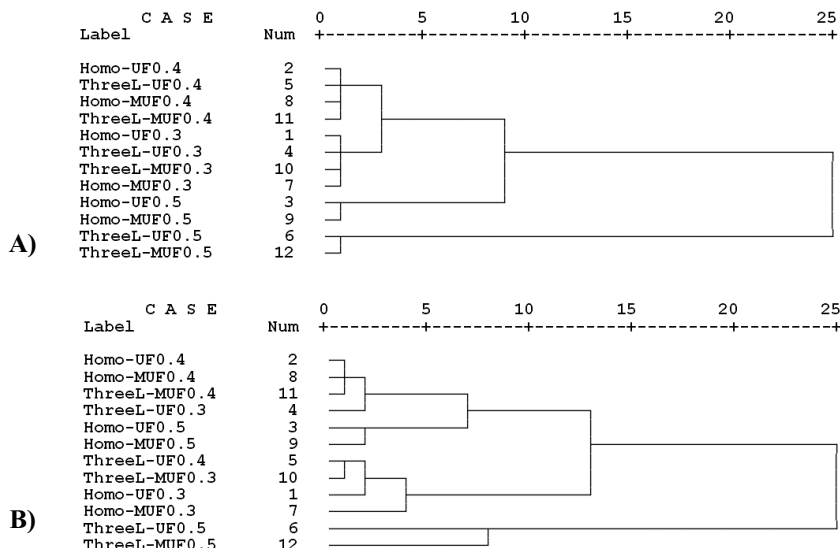


Fig. 7. Cluster analysis of the 12 treatments based on specific gas permeability and the two liquid permeability of 1st-Drop and 50-mm lowering times (A), and based on specific gas and liquid permeability and noise reduction coefficients at the two 500 and 2000 Hz frequencies (B)

(Homo = Homogeneous boards;
ThreeL=Three-Layered boards;
UF = Urea Formaldehyde resin;
MUF = Melamine Urea Formaldehyde resin)

cm³), the type of resin, or the type of boards as homogeneous or three-layered, do not significantly affect the permeability property of the boards. In the higher density boards of 0.5 g/cm³ though, the type of the boards may significantly affect the permeability; however, resin-type still did not show any significant effect on the permeability as the two boards of either homogeneous or three-layered of the same density of 0.5 g/cm³ were closely clustered.

Cluster analysis of the 12 treatments based on the two NRCs (at the frequencies of 500 and 2000 Hz), as well as the specific gas permeability (Gas 5) and the two liquid permeability (1st-Drop and 50-mm lowering times), also showed that the type of boards (homogeneous or three-layered) and the density played more importantly than the type of resin (Figure 7B). In this connection, the sudden change between the layers in the three-layered boards seemed to greatly affect the noise absorption property of the boards; this sudden change in the board-layers, in addition to the increase in the

density, resulted in the three-layered boards with 0.5 g/cm³ of density to be clustered quite differently.

Based on the findings of the present study it may be concluded that specific gas and liquid permeability were significantly influenced by the density. The high R-square between gas and liquid permeability values indicated that the non-destructive test of gas permeability measurement could be considered a suitable criterion for prediction of the liquid permeability behavior in sugar-can particleboards. Furthermore, noise reduction coefficient was mostly affected by the density and board-type (homogeneous and three-layered) rather than the resin type (UF or MUF). Also, resin-type seemed to slightly decrease gas and liquid permeability; however, it did not significantly affect noise reduction coefficient in sugar-cane particleboards.

Conclusions

- Specific gas and liquid permeability values are influenced by the density;
- Gas permeability measurement is a suitable criterion for prediction of the liquid permeability;
- Noise reduction coefficient is mostly affected by the density and board-type;
- Resin-type slightly decreases gas and liquid permeability; however, it does not affect noise reduction coefficient.

Acknowledgments

The authors are grateful to Engr. Peyman Kashani, from the Institute of Standard and Industrial Research of Iran (ISI-RI), for the procurement of the standards. Dr. Reza Hosseinpouria acknowledges the financial contribution of VINNOVA (VINNMR Marie Curie Incoming project 2015-04825)

References

- Ada, R.**, 2013. Cluster analysis and adaptation study for safflower genotypes. *Bulgarian Journal of Agricultural Science*, **19** (1): 103 – 109.
- Arce, N. and R. Moya**, 2015. Wood characterization of adult clones of *Tectona grandis* growing in Costa Rica. *CERNE*, **21** (3): 353-362.
- Awoyemi, L.**, 2007. Determination of optimum borate concentration for alleviating strength loss during heat treatment of wood. *Wood Sci. Tech*, **42**: 39-45.
- Grace, J. K.**, 1996. Susceptibility of compressed bagasse fiber to termite attack. *Forest Products Journal*, **46** (9): 76-78.
- Grace, J. K.**, 2005. Termite response to agricultural fiber composites: Bagasse. The 36th Annual Meeting of IRG/WP 05-10549, Bangalore, India.
- Kelly, M. W.**, 1997. Critical literature review of relationships between processing parameters and physical properties of particleboard. USDA, *For. Ser. Gen. Tech. Rep. FPL*, Madison, v. 10, 66 pp.
- Lei, Y. C., S. J. Liu, J. A. Li and R. C. Sun**, 2010. Effect of hot-water extraction on alkaline pulping of bagasse. *Biotechnology Advances*, **28** (5): 609-612.
- Luz, S. M., A. R. Goncalves, P. M. C. Ferrao, M. J. M. Freitas, A. L. Leao and Jr. A. P. Del Arco**, 2007. Water absorption studies of vegetable fibers reinforced polypropylene composites. In: Proceedings of The 6th Intl. Symposium on Natural Polymers and Composites.
- Maloney, T. M.**, 1993. Modern Particleboard and Dry Process Fiberboard Manufacturing, 2nd ed., San Francisco, *Miller Freeman*, 689 pp.
- Panyakaew, S. and S. Fotios**, 2011. New thermal insulation boards made from coconut husk and bagasse. *Energy and Buildings*, **43** (7): 1732-1739.
- Pereira, P. H. F., H. C. J. Voorwald, M. O. H. Cioffi, D. R. Mulinari, S. M. Da Luz, and M. L. C. P. Da Silva**, 2011. Sugarcane bagasse pulping and bleaching: thermal and chemical characterization. *BioResources*, **6** (3): 2471-2482.
- Ripoli, C. C., Jr. W. F. Molina and M. L. C. Ripoli**, 2000. Energy Potential of sugarcane biomass in Brazil. *Scientia Agricola*, **57** (4): 677-681.
- Lei, Y. C., S. J. Liu, J. A. Li and R. C. Sun**, 2010. Effect of hot-water extraction on alkaline pulping of bagasse. *Biotechnology Advances*, **28** (5): 609-612.
- Rainey, T. J., W. O. S. Doherty, D. M. Martinez, R. J. Brown and N. A. Kelson**. 2009. An experimental study of Australian sugarcane bagasse pulp permeability. *Appita Journal*, **62** (4): 296-302.
- Rowell, R. M. and F. J. Keanny**, 1991. Fiberboards made from acetylated bagasse fiber. *Wood and Fiber Science*, **23** (1): 15-22.
- Rowell, R. M., J. S. Han and J. S. Rowell**, 2000. Characterization and factors affecting fiber properties. In: E. Frollini, A. L. Leao, and L. H. C. Mattoso (Eds), *Natural Polymers and Agrofibers Based Composites*, *Embrapa Instrumentacao Agropecuaria Ed.*, Sao Carlos-SP, Section II – Agrofibers Composites, pp. 115-134.
- Siau J. F.**, 1995. Wood: Influence of Moisture on Physical Properties. Blacksburg, VA, Department of Wood Science and Forest Products, *Virginia Polytechnic Institute and State University*, pp. 1-63.
- Sousa, N. VdO, T. V. Carvalho, S. B. Honorato, C. L. Gomes, F. C. F. Barros, M. A. Araujo-Silva, Freire P. T. C. and R. F. Nascimento**, 2012. Coconut bagasse treated by thiourea/ammonia solution for cadmium removal: Kinetics and adsorption equilibrium. *BioResources*, **7** (2): 1504-1524.
- Stockel, F., J. Konnerth, J. Moser, W. Kantner and W. Gindl-Altmutter**, 2012. Micromechanical properties of the interphase in pMDI and UF lines. *Wood Science and Technology*, **46**: 611-620, DOI 10.1007/s00226-011-0432-0.
- Sun, J. X., X. F. Sun, H. Zhao and R. C. Sun**, 2004. Isolation and characterization of cellulose from sugarcane bagasse. *Polym. Degrad. Stab.*, **84**: 331-339.
- Taghiyari, H. R.**, 2012. Fire-retarding properties of nano-silver in

- solid woods. *Springer: Wood Sci. Technol.*, **46** (4): 939-952, DOI 10.1007/s00226-011-0455-6.
- Taghiyari, H. R., M. Layeghi and F. A. Liyafouee**, 2012. Effects of dry ice on gas permeability of nano-silver-impregnated *Populus nigra* and *Fagus orientalis*. *IET Nanobiotechnology*. Doi: 10.1049/iet.nbt.2011.0048.
- Taghiyari, H. R. and B. M. Malek**, 2014. Effect of heat treatment on longitudinal gas and liquid permeability of circular and square-shaped native hardwood specimens. *Heat and Mass Transfer*, DOI 10.1007/s00231-014-1319-z.
- Taghiyari, H. R., E. Bari, O. Schmidt, M. A. T. Ghanbari, A. Karimi and P. M. D. Tahir**, 2014. Effects of nanowollastonite on biological resistance of particleboard made from wood chips and chicken feather against *Antrodia vaillantii*. *International Biodeterioration & Biodegradation*, **90**: 93-98.
- Taghiyari, H. R., H. Rangavar and O. F. Bibalan**, 2011. Nano-silver in particleboard. *BioResources*, **6** (4): 4067-4075.
- Tsuchikawa, S.**, 2007. A review of recent near infrared research for wood and paper. *Applied Spectroscopy Reviews*, **42**: 43-71.
- Valenzuela, J., E. von Leyser, A. Pizzi, C. Westermeyer and B. Gorriini**, 2012. Industrial production of pine tannin-bonded particleboard and MDF. *European Journal of Wood and Wood Products*, **70** (5): 735-740.
- Wu, Q.**, 2003. Particleboard from sugarcane bagasse for value-added applications. *Louisiana Agriculture*, **46** (3): 11.
- Youngquist, J. A., A. M. Krzysik, B. W. English, H. N. Spelter and P. Chow**, 1996. Agricultural fibers for use in building components. In: The Use of Recycled Wood and Paper in Building Applications. Forest Products Society Proceedings 7386. *Forest Products Society*, Madison, Wisconsin, pp. 123-134.

Received July, 29, 2016; accepted for printing June, 9, 2017